

Analyses of Spectral Behaviors of Semiconductor Lasers under Weak Optical Injection Locked to External Light Injected

Jung-Tae Kim, *Member, KIMICS*

Abstract— We have investigated the spectral characteristics of semiconductor lasers locked to the external light injected from a modulated laser. Our study on FM sideband injection locking has shown that when SLs are locked to the target sidebands of the directly modulated ML, the presence of the unselected sidebands influences the resulting microwave signals. The unselected signals can produce the unwanted beat signals around the desired beat signal, which degrade the overall system performance. This analysis gives way to generate Giga HZ signal generation.

Index Terms— Semiconductor lasers, Current-modulated lasers, Optical weak injection locking, Spectral characteristics

I. INTRODUCTION

The optical injection locking technique with semiconductor laser diodes (LDs) is widely used in chirp and linewidth reduction, [1] measurement of the laser dynamics, [2, 3] wavelength conversion, [4] and optical microwave generation. [5-7] In particular, the optical microwave signal generation technique with injection locked lasers is very promising for many applications because it can easily produce high frequency signals with low phase noise. In the sideband injection-locking scheme, [5-7] the master laser (ML) is electrically modulated and two of the resulting sidebands having the desired frequency separation are injected into two slave lasers (SLs). When these two injection-locked SLs beat each other in the photodiode (PD), the desired microwave signal is generated. Using this method, Braun et al. has recently reported the successful demonstration of 60GHz beat signal generation. [6, 7]

Manuscript received August 17, 2009 ; revised September 8, 2009. Jung Tae Kim is with the Department of Electronic Engineering, Mokwon University, Taejon, 302-729, Korea (Tel: +82-42-829-7657, Fax: +82-42-823-8506, Email: jtkim3050@mokwon.ac.kr)

Our recent study on FM sideband injection-locking has shown that when SLs are locked to the target sidebands of the directly modulated ML, the presence of the unselected sidebands influence the resulting microwave signals.[8] The unselected sidebands can produce the unwanted beat signals around the desired beat signal, which degrade the overall system performance. The reduction in the incident light power helps in suppressing the unwanted beat signals, but it also reduces the locking range causing the stability problem.

In this paper, we investigate the influence of the ML sidebands on the spectral characteristics of sideband injection-locked semiconductor lasers numerically and experimentally. The numerical models for the sideband injection-locked slave lasers are based on extended Lang's model, which includes the influence of multiple ML sidebands expressed by the Bessel function.[9-11] The large-signal analyses for the SL spectra with multiple ML sidebands are performed. Finally, we investigate the influence of the unselected sidebands on the SL spectral properties for the different ML injection powers.

II. THEORY

2.1 OPTICAL INJECTION LOCKING

Synchronization approach is appropriate for the conventional protocol because of its design for simple RFID implementation.

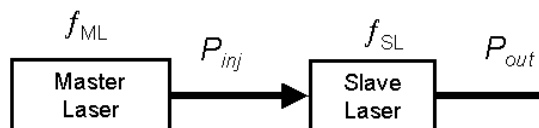


Fig. 1 Basic optical injection locking configuration

The optical injection locking configuration is made up of ML and SL as shown in Fig. 1, where the CW ML light is injected into the SL cavity. Two lasers have a frequency offset of Δf , where Δf is defined as $f_{ML} - f_{SL}$. It is assumed that the injected ML light has the same polarization as SL by the proper control of

the polarization controller located between two lasers. Assuming DFB lasers with negligible sidemodes are used for both ML and SL, the SL under the influence of external light injection can be described by the following single-mode rate-equations. [12]

$$\frac{dP}{dt} = \left[\frac{\Gamma g_0}{1 + \varepsilon P} (N - n_s) - \frac{1}{\tau_p} \right] P + \frac{\Gamma \beta}{\tau_n} N + 2K_C \sqrt{P_{in} P} \cos(\Phi_{ML} - \Phi) \quad (2-a)$$

$$\frac{d\Phi}{dt} = -2\pi \Delta f + \frac{1}{2} \alpha \left[\frac{\Gamma g_0}{1 + \varepsilon P} (N - n_s) - \frac{1}{\tau_p} \right] + K_C \sqrt{\frac{P_{in}}{P}} \sin(\Phi_{ML} - \Phi) \quad (2-b)$$

$$\frac{dN}{dt} = \frac{I}{qV_a} - \frac{g_0}{1 + \varepsilon P} (N - n_s) P - \frac{N}{\tau_n} \quad (2-c)$$

In the above equations, P_{in} and Φ_{ML} represent the density and the phase of the injected photons and K_C ($= \nu_g/2L_a$) the coupling rate between ML and SL. Other parameters have the usual meanings. The numerical values for the laser parameters used are obtained from Ref. 13.[13] From the steady-state analysis of the rate-equations, Fig. 2 shows the locking and unlocking regions as function of Δf and R . Here, injection power ratio R is defined as P_{inj} / P_{out} , where P_{inj} is the injected optical power just outside the SL facet and P_{out} is SL output power. For the results shown in Fig. 2, SL output power is fixed at 2 mW. If the gain suppression and the spontaneous emission terms are ignored, the range of Δf that allows locking can be determined as follows. [14]

$$|\Delta f (= f_{ML} - f_{SL})| \leq \frac{K_C}{2\pi} \sqrt{\frac{P_{in}}{P} (1 + \alpha^2)} \quad (3)$$

This locking range can be further classified into two distinctive regimes: stable-locking and unstable-locking. In the stable-locking regime, the output power converges to a steady-state value when a small perturbation is introduced. In the unstable locking regime, however, the power does not converge to the steady-state value but experiences a self-sustained oscillation or even chaos when a small perturbation is introduced. [14] Such an oscillation and chaos produce multiple sidebands in the output optical spectra. The range for the stable-locking regime can be determined by the s-domain stability analysis of the linearized rate-equations above. The shaded area inside the unstable locking regime in Fig. 2 represents the place where the chaos occurs. The chaos area outside the locking regimes is not taken into account, here. The asymmetry of the stable-locking regime is dependent on R . The center of the stable-locking bandwidth is shifted toward the shorter frequency from the SL lasing frequency with increasing R .

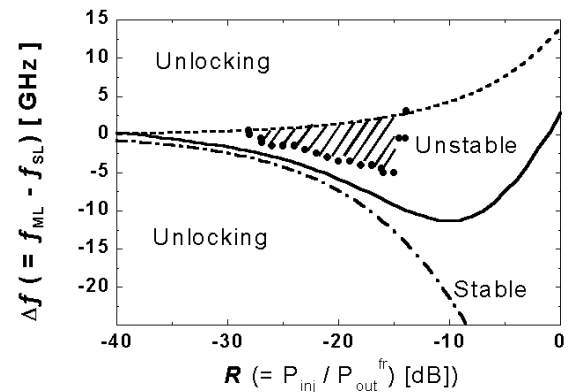


Fig. 2 Locking regime

2.2 LOCKING RANGE

When the semiconductor laser is directly modulated, it is intensity-modulated (IM) and frequency-modulated (FM) simultaneously due to the presence of the intrinsic frequency chirp. To a first approximation, the optical output of the directly modulated semiconductor laser can be expressed by the following complex electric field. [9-11]

$$\tilde{E} = P_0^{1/2} (1 + m_{IM} \cos(\Omega_m t + \Phi_{IM}))^{1/2} e^{j m_{FM} \sin(\Omega_m t + \Phi_{FM})} \quad (4)$$

P_0 means the average output power, Ω_m is the applied angular modulation frequency, m_{IM} and m_{FM} are the IM and FM indices, respectively. And, Φ_{IM} and Φ_{FM} are the corresponding phases. Eq. (4) shows that a directly modulated semiconductor laser has the sidebands at the harmonics of the modulation frequency in the electrical field spectrum. The electrical field in Eq. (3) can be expressed by a series of Bessel functions as follows, [9-11]

$$\tilde{E} = P_0^{1/2} \sum_{k=-\infty}^{\infty} C_k e^{jk(\Omega_m t + \Phi_{IM})} \quad (5-a)$$

$$C_k = e^{jk\Delta\Phi} \left[J_k(m_{FM}) + \frac{m_{IM}}{4} (J_{k+1}(m_{FM}) e^{j\Delta\Phi} + J_{k-1}(m_{FM}) e^{-j\Delta\Phi}) \right] \quad (5-b)$$

Where, $\Delta\Phi$ is the phase difference between Φ_{FM} and Φ_{IM} . When the applied modulation frequency, Ω_m , is given, the modulation indices and phases in Eq. (5) can be analytically determined from the IM and FM responses of the linearized laser rate-equations in Eq (1), where no external light injection is included, that is, $P_{in} = 0$. [10]

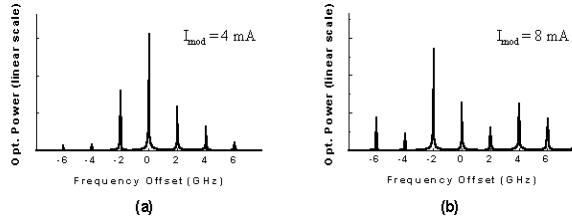


Fig. 3 Dependence of the optical spectrum for the different modulation powers

The complex electrical amplitude of each sideband of the directly modulated semiconductor laser can be denoted in (4-b). Eq. (4-b) shows the asymmetric sidebands in the optical spectrum, since the IM response is superimposed on the FM response. [9-10] The magnitude and quantity of the sidebands are determined directly by the FM index, m_{FM} , which has the relation with the intrinsic laser frequency chirp and increases with the modulation current. The increase of m_{FM} can make the target sideband power increased so that its power becomes larger than the center lasing peak power in the optical spectrum as illustrated in Fig. 3. In Fig. 3, it is assumed that the LD is biased at 1.5 times threshold at the modulation frequency of 2 GHz.

III. CHARACTERISTICS OF INJECTION LOCKING

This chapter deals with the characteristics of injection locking for semiconductor lasers by large signal and spectra analysis. Figure 4 shows a basic injection-locking configuration. Optical power from Master laser goes through isolator and is injected to slave laser. We use laser diode parameters in reference and single mode Van der Pol equation to model numerical injection-locking method [9]. Boundary condition of locking region in steady state is as follows [11].

$$\begin{aligned} \Delta\omega &= 2\pi(f_{ML} - f_{SL}) \\ &= K_c \sqrt{\frac{S_{ML}}{S_{SL}}} (\sin\theta - \alpha \cos\theta) \end{aligned} \quad (6)$$

K_c is coupling coefficient, S_{ML} is photon density injected from ML (Master Laser) to SL (Slave Laser), S_{SL} is photon density in SL cavity, and θ is a phase difference between ML and SL. By analyzing small signal analysis in given rate equation, all zeros are located in left s-domain to lock statically stable in 3rd order system function. We have been showed values to satisfy stability analysis in Fig. 4. From the figures, it

is divided into stable-locking, unstable locking and unlocked region. We can expect signal response and spectrum given values in Fig. 4. In the case of signal response, waveform is depicted under injected step-like current from $1.01I_{th}$ to $1.5I_{th}$ at 2ns. Waveforms by FFT transformation after deriving portion of steady state at the window after overshoot transient response are shown in Fig. 4-3. Each value is normalized by high values obtained from FFT outputs in the case of free-running state. We can estimate all optical power of SL locked in ML frequency in stable locking. The theoretical power spectra were calculated by taking the fast Fourier Transform (FFT) of the steady-state slave intracavity electric field over a given time window. In the case of unstable locking, we can define locked state in a wide expression but power in locked state is vibrating in the center of steady state and it is not stable locked as shown in Fig. 5(c) because unlocked power is not in this state. Spectrum of sideband in Fig. 5(c) stems from relaxation oscillation sideband. In the case of unlocked state, power reaches in constant steady state as unlocked power is increased contrary to the reduction of power of ML frequency in locked state.

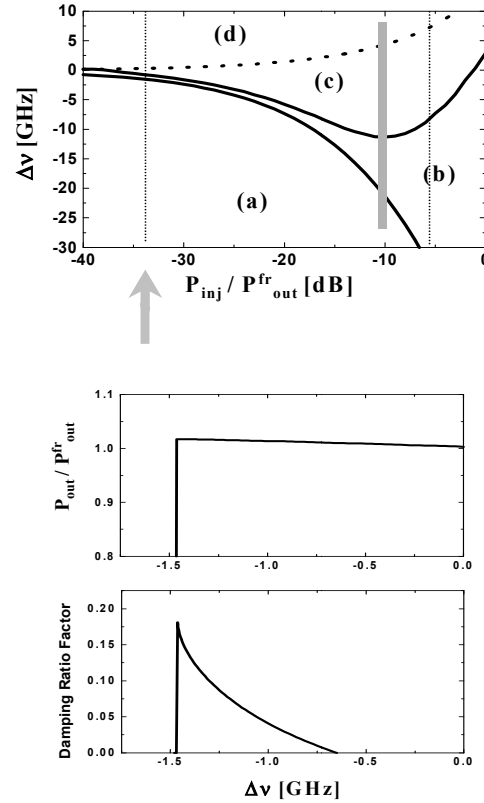
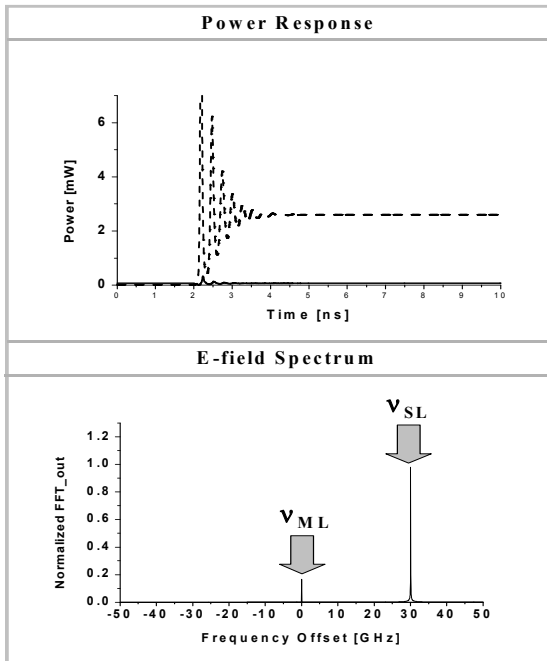
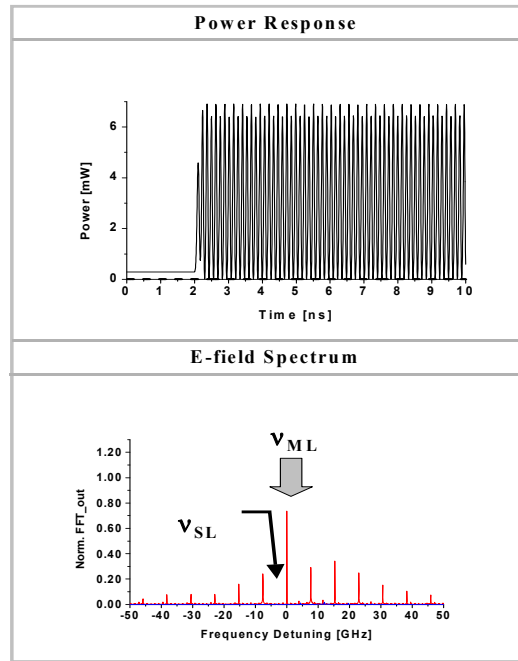


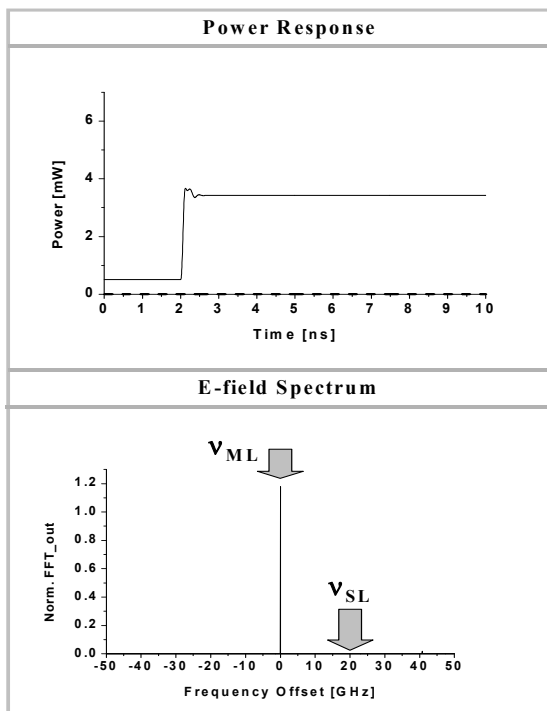
Fig. 4 Locking characteristics of weak optical injection



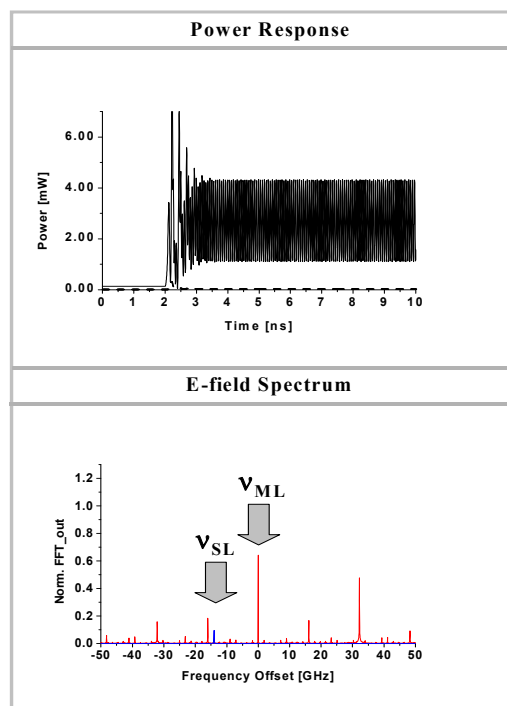
(a) Unlocked(Lower)



(c) Unstable



(b) Stable



(d) Unstable (Upper)

Fig. 5 Power response and E field spectrum in locking condition.

IV. CONCLUSION

We have investigated the spectral characteristics of the semiconductor lasers locked to the sidebands of the master laser, which were expressed by a series of the Bessel function. The numerical model for the semiconductor lasers based on the typical Lang's equation has been extended in order to take into account the simultaneous injection of the multiple sidebands of the directly modulated ML. The numerical simulations have showed that the unselected sidebands can affect the optical and RF-spectral characteristics even when the semiconductor laser is stable-locked to the target sidebands. Due to the presence of the unselected sidebands, the unwanted powers in the optical and RF-spectra will increase with the ML power, and be combined with the fiber chromatic dispersion so that they may degrade the overall system performance.

REFERENCES

- [1] C. Lin, and F. Mengel, "Reduction of frequency chirping and dynamic linewidth in high-speed directly modulated semiconductor lasers by injection locking," *Electron. Lett.*, vol. 20, pp. 1073-1075, 2004.
- [2] C. B. Su, J. Eom, C. H. Lange, C. B. Kim, R. B. Lauer, W. C. Rideout, and J. S. LaCourse, "Characterization of the dynamics of semiconductor lasers using optical modulation," *IEEE J. Quant. Electron.*, vol. 28, pp. 118-127, 2002.
- [3] C. H. Lange, J. Eom, and C. B. Su, "Measurement of intrinsic frequency response of semiconductor lasers using optical modulation," *Electron. Lett.*, vol. 24, pp. 1132-1132, 2008.
- [4] K. Inoue, and N. Takato, "Wavelength conversion for FM light using light injection induced frequency shift in DFB-LD," *Electron. Lett.*, vol. 25, pp. 1360-1362, 1999.
- [5] L. Goldberg, H. F. Taylor, and J. F. Weller, "FM sideband injection of diode lasers," *Electron. Lett.*, vol. 18, pp. 1019-1020, 2002.
- [6] R. -P. Braun, G. Grosskopf, R. Meschenmoser, D. Rohde, G. Schmidt, and G. Villino, "Microwave generation for bidirectional broadband mobile communications using optical sideband injection locking," *Electron. Lett.*, vol. 33, pp. 1395-1394, 2007.
- [7] R. -P. Braun, G. Grosskopf, D. Rohde, and F. Schmidt, "Low-phase-noise millimeter-wave generation at 64 GHz and data transmission using optical sideband injection locking," *IEEE Photon. Technol. Lett.*, vol. 10, pp. 728-730, 2008.
- [8] R. Lang, "Injection locking properties of a semiconductor laser," *IEEE J. Quant. Electron.*, vol. 18, pp. 976-983, 2002.
- [9] S. Kobayashi, Y. Yamamoto, M. Ito, and T. Kimura, "Direct frequency modulation in AlGaAs semiconductor lasers," *IEEE J. Quant. Electron.*, vol. 18, pp. 582-595, 2002.
- [10] G. P. Agrawal, "Power spectrum of directly modulated single-mode semiconductor lasers: chirp-induced fine structure," *IEEE J. Quant. Electron.*, vol. 21, pp. 680-686, 2005.
- [11] E. Peral and A. Yariv, "Large-signal theory of the effect of dispersive propagation on the intensity modulation response of semiconductor lasers," *J. Lightwave Technol.*, vol. 18, pp. 84-89, 2000.
- [12] O. Lidoine, P. B. Gallion, and D. Erasme, "Modulation properties of an injection-locked semiconductor laser," *IEEE J. Quant. Electron.*, vol. 27, pp. 344-351, 2007.
- [13] J. C. Cartledge and G. S. Burley, "The effect of laser chirping on lightwave system performance," *J. Lightwave Technol.*, vol. 7, pp. 568-573, 1999.
- [14] J. Troger, P.-A. Nicati, L. Thevenaz, and Ph. A. Robert, "Novel measurement scheme for injection-locking experiments," *IEEE J. Quant. Electron.*, vol. 35, pp. 32-38, 2009.



Jung-Tae Kim

received his Ph.D. degrees in Electrical and Electronic Engineering from the Yonsei University in 2001. From 1991 to 1996, he joined at ETRI, where he worked as senior member of technical staff. In 2002, he joined the department of electronic engineering, Mokwon University, Korea, where he is presently professor. His research interest is in the area of information optical security technology that includes network security system design, USN and wireless security protocol.